

# Photoinduced $\eta$ -pairing in the Hubbard Model

Tatsuya Kaneko<sup>1</sup>, Tomonori Shirakawa<sup>2,1,3,4</sup>, Sandro Sorella<sup>2,5,3</sup>, and Seiji Yunoki<sup>1,3,4</sup>

<sup>1</sup>Computational Condensed Matter Physics Laboratory,

RIKEN Cluster for Pioneering Research (CPR), Wako, Saitama 351-0198, Japan

<sup>2</sup>SISSA–International School for Advanced Studies, Via Bonomea 265, 34136 Trieste, Italy

<sup>3</sup>Computational Materials Science Research Team,

RIKEN Center for Computational Science (R-CCS), Kobe, Hyogo 650-0047, Japan

<sup>4</sup>Computational Quantum Matter Research Team,

RIKEN Center for Emergent Matter Science (CEMS), Wako, Saitama 351-0198, Japan

<sup>5</sup>Democritos Simulation Center CNR–IOM Instituto Officina dei Materiali, Via Bonomea 265, 34136 Trieste, Italy

(Dated: November 17, 2022)

Superconductivity is one of the most fascinating quantum states of matter and the search for new unconventional superconductivity has been at the forefront of the research of strongly correlated materials. Here, by employing unbiased numerical methods, we show that pulse irradiation can induce unconventional superconductivity even in the Mott insulator of the Hubbard model. The superconductivity found here in the photo-excited state is due to the  $\eta$ -pairing mechanism, characterized by staggered pair-density-wave oscillations in the off-diagonal long-range correlation. Because of the selection rule, we show that the non-linear optical response is essential to increase the number of  $\eta$ -pairs and thus enhance the superconducting correlation in the photo-excited state. Our finding demonstrates that non-equilibrium many-body dynamics is an alternative pathway to access a new exotic quantum state that is absent in the ground state phase diagram.

Recent experiments have clearly demonstrated that the non-equilibrium dynamics can induce many intriguing phenomena in condensed-matter materials [1–5]. Among them, the most striking is the discovery of photoinduced transient superconducting behaviors in some of high- $T_c$  cuprates [6–8] and alkali-doped fullerenes [9, 10]. It has also been theoretically shown that superconductivity can be enhanced or induced by pulse irradiation in models for these materials [11–14]. In these studies, the main focus is a photoinduced state with physical properties already present in the corresponding equilibrium phases. In the case of Mott insulator (MI), photoinduced insulator-to-metal transitions have been reported in time-resolved experiments for several transition-metal and organic-molecular compounds [15–19]. In the MI, the photoinduced metallic state has been recognized as a results of photo-carrier doping by creating doublon-holon pairs with no peculiar electronic states emerging [20–22].

Here, we show that the pulse irradiation can induce superconductivity even in the celebrated MI of the Hubbard model. The photoinduced superconductivity is due to the  $\eta$ -pairing mechanism, forming on-site singlet pairing that exhibits, unlike conventional  $s$ -wave superconductivity, the staggered off-diagonal long-range correlation with a phase of  $\pi$ . Because of the selection rule, the non-linear optical response is essential to increase the number of  $\eta$ -pairs and thus enhance the superconducting correlation. The superconductivity found here is absent in the ground state phase diagram and is induced neither by a change of the effective interaction of the Hubbard model nor the simple photo-carrier doping. Therefore, our finding opens a conceptually different possibility of unraveling and controlling excited states with intriguing properties by non-equilibrium many-body quantum dynamics, and also provides an alternative mechanism for enhancing superconductivity.

To demonstrate that superconductivity can be photoinduced in a Mott insulator, here we consider the half-filled one-dimensional (1D) Hubbard model at zero temperature. However, our finding does not depend on the spatial dimensionality (see Supplemental Material for two dimensional case [23]). The model is described by the following Hamiltonian:

$$\hat{\mathcal{H}} = -t_h \sum_{i,\sigma} \left( \hat{c}_{i,\sigma}^\dagger \hat{c}_{i+1,\sigma} + \text{H.c.} \right) + U \sum_i \hat{n}_{i,\uparrow} \hat{n}_{i,\downarrow}, \quad (1)$$

where  $\hat{c}_{i,\sigma}$  ( $\hat{c}_{i,\sigma}^\dagger$ ) is the annihilation (creation) operator for an electron at site  $i$  with spin  $\sigma$  ( $=\uparrow, \downarrow$ ) and  $\hat{n}_{i,\sigma} = \hat{c}_{i,\sigma}^\dagger \hat{c}_{i,\sigma}$ .  $t_h$  is the hopping integral between the nearest neighboring sites and  $U$  ( $> 0$ ) is the on-site repulsive interaction. At half-filling, the ground state of the repulsive 1D Hubbard model is the MI with strong antiferromagnetic correlations.

A time( $t$ )-dependent external field is introduced via the Peierls phase in the first term of Eq. (1) by  $t_h \hat{c}_{i,\sigma}^\dagger \hat{c}_{i+1,\sigma} \rightarrow t_h e^{iA(t)} \hat{c}_{i,\sigma}^\dagger \hat{c}_{i+1,\sigma}$  [24], where  $A(t)$  is the time-dependent vector potential, and the light velocity  $c$ , the elementary charge  $e$ , the Planck constant  $\hbar$ , and the lattice constant are set to one. We consider a pump pulse given as  $A(t) = A_0 e^{-(t-t_0)^2/(2\sigma_p^2)} \cos[\omega_p(t-t_0)]$  with the amplitude  $A_0$ , the frequency  $\omega_p$ , and the pulse width  $\sigma_p$  centered at time  $t_0$  ( $> 0$ ) [25–29]. With finite external field  $A(t)$ , the Hamiltonian becomes time-dependent,  $\hat{\mathcal{H}} \rightarrow \hat{\mathcal{H}}(t)$ , and the equilibrium ground state of  $\hat{\mathcal{H}}$  at  $t = 0$  evolves in time, which is indicated here by  $|\Psi(t)\rangle$ . We employ the time-dependent exact diagonalization (ED) method for a finite-size cluster of  $L$  (even) sites with periodic boundary conditions (PBC) to solve the time-dependent Schrödinger equation [23]. We set the hopping integral  $t_h$  ( $t_h^{-1}$ ) as unit of energy (time) and the total

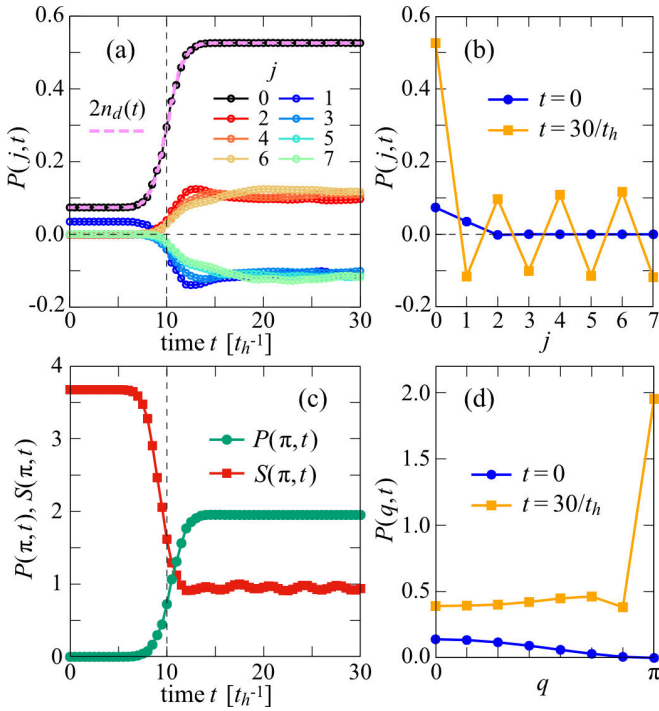


Figure 1. (a) Time evolution of the on-site pair correlation function  $P(j, t)$ . For comparison, the double occupancy  $n_d(t)$  is also shown by the pink dashed line. (b)  $P(j, t)$  at  $t = 0$  (blue circles) and  $t = 30/t_h$  (orange squares). (c) Time evolution of the on-site pair structure factor  $P(q, t)$  (green circles) and the spin structure factor  $S(q, t)$  (red squares) at  $q = \pi$ . (d)  $P(q, t)$  at  $t = 0$  (blue circles) and  $t = 30/t_h$  (orange squares). The results are calculated by the ED method for  $L = 14$  at  $U = 8t_h$ .  $A(t)$  is adopted with  $A_0 = 0.4$ ,  $\omega_p = 8.2t_h$ ,  $\sigma_p = 2/t_h$ , and  $t_0 = 10/t_h$ .

number  $N$  of electrons to be  $L$  at half-filling.

Enhancement of the double occupancy  $n_d(t) = \frac{1}{L} \sum_i \langle \Psi(t) | \hat{n}_{i,\uparrow} \hat{n}_{i,\downarrow} | \Psi(t) \rangle$  has been already reported in photo-excited states of the MIs [28, 30–32]. Here, we find a significant increase of the superconducting pair correlation for the on-site singlet pair  $\hat{\Delta}_i = \hat{c}_{i,\uparrow} \hat{c}_{i,\downarrow}$  after the pulse irradiation in the MI. Figure 1(a) shows the time evolution of the real-space pair correlation function defined as  $P(j, t) = \frac{1}{L} \sum_i \langle \Psi(t) | (\hat{\Delta}_{i+j}^\dagger \hat{\Delta}_i + \text{H.c.}) | \Psi(t) \rangle$ . Notice that  $P(j, t)$  at  $j = 0$  corresponds to the double occupancy, i.e.,  $P(j=0, t) = 2n_d(t)$ . We thus confirm the enhancement of the double occupancy  $n_d(t)$  by the pulse irradiation. Surprisingly,  $P(j \neq 0, t)$  is also enhanced significantly by the pulse irradiation and oscillates with the opposite phases between odd and even sites.

As shown in Fig. 1(b), the pair correlation after the pulse irradiation extends to longer distances over the cluster, while the pair correlation is essentially absent in the initial MI state before the pulse irradiation. It is also clear that the sign of  $P(j, t)$  alternates between neighboring sites, similar to a density wave, and accordingly the pair structure factor  $P(q, t) = \sum_j e^{iqR_j} P(j, t)$ ,

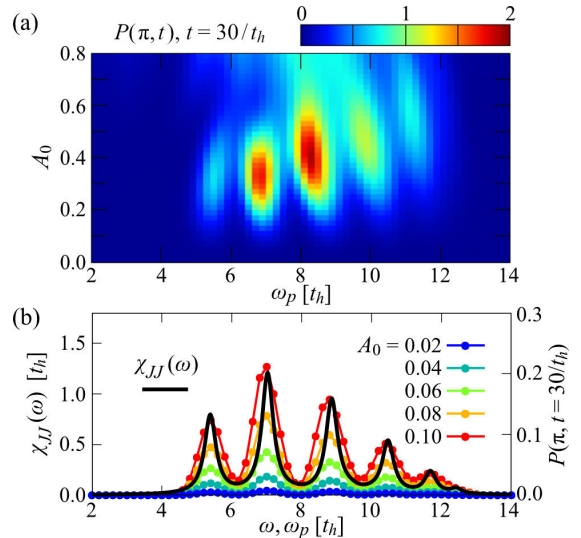


Figure 2. (a) Contour plot of the pair structure factor  $P(q = \pi, t)$  at  $t = 30/t_h$  with varying  $\omega_p$  and  $A_0$ . (b) The ground state optical spectrum  $\chi_{JJ}(\omega)$  is compared with  $P(q = \pi, t = 30/t_h)$  as a function of  $\omega_p$  for different values of  $A_0$ . The results are calculated by the ED method for  $L = 14$  at  $U = 8t_h$  with  $\sigma_p = 2/t_h$  and  $t_0 = 10/t_h$ .

where  $R_j$  is the location of site  $j$ , shows a sharp peak at  $q = \pi$  [see Fig. 1(d)]. The time evolution of  $P(q, t)$  and the spin structure factor  $S(q, t)$  [33] is also calculated at  $q = \pi$  in Fig. 1(c). The antiferromagnetic correlation  $S(\pi, t)$  is suppressed by the pulse irradiation, while the pair correlation  $P(q = \pi, t)$  is strongly enhanced despite that it is exactly zero before the pulse irradiation. As shown in Supplemental Material [23], our matrix product state calculations also find the large enhancement of the pair correlation even for larger chains that cannot be treated by the ED method.

In order to identify the optimal control parameters for the enhancement of  $P(q = \pi, t)$ , Fig. 2(a) shows the contour plot of  $P(\pi, t)$  after the pulse irradiation with different values of  $A_0$  and  $\omega_p$ . Although the figure refers to  $P(\pi, t)$  at  $t = 30/t_h$ , the values are almost identical with the time-averaged ones between  $20/t_h \leq t \leq 30/t_h$ . For small  $A_0$ , we find that the peak structure of  $P(q = \pi, t)$  as a function of  $\omega_p$  are essentially the same as the ground-state optical spectrum given by  $\chi_{JJ}(\omega) = \frac{1}{L} \langle \psi_0 | \hat{J} \delta(\omega - \hat{\mathcal{H}} + E_0) \hat{J} | \psi_0 \rangle$ , where  $|\psi_0\rangle$  is the ground state of  $\hat{\mathcal{H}}$  with its energy  $E_0$  and  $\hat{J} = it_h \sum_{i,\sigma} (\hat{c}_{i+1,\sigma}^\dagger \hat{c}_{i,\sigma} - \hat{c}_{i,\sigma}^\dagger \hat{c}_{i+1,\sigma})$  is the current operator [see Fig. 2(b)]. This agreement is highly non-trivial and the reason will be clear in the later discussion.  $P(q = \pi, t)$  after the pulse irradiation is the highest at  $A_0 \sim 0.4$  and  $\omega_p \sim 8t_h$  ( $= U$ ). We should emphasize that the enhancement of  $P(q = \pi, t)$  cannot be explained simply by photo-doping of carriers into the MI or due to a dynamical phase transition induced by effectively varying the model parameters because there is no region in the ground state phase diagram of the Hubbard

model, showing large on-site pairing correlations.

Instead, the behavior of the on-site pairs in the photoinduced state shown in Fig. 1 can be understood in terms of the so called  $\eta$ -pairing, a concept originally introduced by Yang [34]. In order to define the  $\eta$ -pairing, let us first introduce the following operators:  $\hat{\eta}_j^+ = (-1)^j \hat{c}_{j,\downarrow}^\dagger \hat{c}_{j,\uparrow}^\dagger$ ,  $\hat{\eta}_j^- = (-1)^j \hat{c}_{j,\uparrow} \hat{c}_{j,\downarrow}$ , and  $\hat{\eta}_j^z = \frac{1}{2}(\hat{n}_{j,\uparrow} + \hat{n}_{j,\downarrow} - 1)$ . Notice that  $\hat{\eta}_j^\pm$  is the same as  $\hat{\Delta}_j^{(\dagger)}$  except for the phase factor. We can now easily show that these operators satisfy the  $SU(2)$  commutation relations, i.e.,  $[\hat{\eta}_j^+, \hat{\eta}_j^-] = 2\hat{\eta}_j^z$  and  $[\hat{\eta}_j^z, \hat{\eta}_j^\pm] = \pm\hat{\eta}_j^\pm$ . Similarly, the total  $\hat{\eta}$ -operators,  $\hat{\eta}^\pm = \sum_j \hat{\eta}_j^\pm$  and  $\hat{\eta}_z = \sum_j \hat{\eta}_j^z$ , satisfy the  $SU(2)$  commutation relations. The essential property of the  $\hat{\eta}$ -operators, relevant to the following discussion, is that they also satisfy  $[\hat{\mathcal{H}}, \hat{\eta}^\pm] = \pm U \hat{\eta}^\pm$  with the Hubbard Hamiltonian  $\hat{\mathcal{H}}$  in Eq. (1).

Yang originally proposed the  $\eta$ -pairing state  $|\phi_{N_\eta}\rangle \propto (\hat{\eta}^+)^{N_\eta} |0\rangle$ , where  $|0\rangle$  is the vacuum state with no electrons and  $N_\eta$  is the number of  $\eta$ -pairs [34]. Yang's  $\eta$ -pairing state  $|\phi_{N_\eta}\rangle$  has two remarkable properties [34]. First,  $|\phi_{N_\eta}\rangle$  is an exact eigenstate of the Hubbard model with  $2N_\eta$  electrons, satisfying  $\hat{\mathcal{H}}|\phi_{N_\eta}\rangle = N_\eta U |\phi_{N_\eta}\rangle$ . Second,  $\langle \phi_{N_\eta} | \hat{\Delta}_i^\dagger \hat{\Delta}_j | \phi_{N_\eta} \rangle = \frac{N_\eta(L-N_\eta)}{L(L-1)} e^{i\pi(R_i-R_j)}$  for  $i \neq j$ , indicating  $|\phi_{N_\eta}\rangle$  has off-diagonal long-range order. Notice that both Yang's  $\eta$ -pairing state  $|\phi_{N_\eta}\rangle$  and our photoinduced state  $|\Psi(t)\rangle$  show similar sign alternating characters in the pair correlation function. However, the photoinduced state  $|\Psi(t)\rangle$  excited from the MI state should be different from the  $\eta$ -pairing state  $|\phi_{N_\eta}\rangle$ , because all the occupied sites in  $|\phi_{N_\eta}\rangle$  are doubly occupied by electrons. In fact, we have confirmed numerically that  $|\langle \phi_{N_\eta} | \Psi(t) \rangle|^2 = 0$  at  $t = 30/t_h$ .

As a candidate of the photoinduced state which shows large  $P(q = \pi, t)$ , we now consider the eigenstate generated from the lowest weight state (LWS) for  $\hat{\eta}$ -operators. For this purpose, it is important to notice that  $[\hat{\mathcal{H}}, \hat{\eta}^+ \hat{\eta}^-] = [\hat{\mathcal{H}}, \hat{\eta}_z] = 0$ . Therefore, any eigenstate of the Hubbard Hamiltonian  $\hat{\mathcal{H}}$  is also the eigenstate  $|\eta, \eta_z\rangle$  of  $\hat{\eta}^2$  and  $\hat{\eta}_z$  with the eigenvalues  $\eta(\eta+1)$  and  $\eta_z$ , respectively, where  $\hat{\eta}^2 = \frac{1}{2}(\hat{\eta}^+ \hat{\eta}^- + \hat{\eta}^- \hat{\eta}^+) + \hat{\eta}_z^2$ ,  $\eta = 0, 1, 2, \dots, \frac{L}{2}$  (at half-filling with the same number of up and down electrons  $N_\uparrow = N_\downarrow$ ) and  $\eta_z = -\eta, -\eta+1, \dots, \eta$ . This is precisely the analogue to the total spin operator  $\hat{S}$  and its  $z$  component  $\hat{S}_z$  characterizing any eigenstate of  $\hat{\mathcal{H}}$  with  $|S, S_z\rangle_{\text{spin}}$ . The LWS is  $|\eta, \eta_z = -\eta\rangle$  and thus satisfies  $\hat{\eta}^- |\eta, -\eta\rangle = 0$ . Remarkably, Essler *et al.* have shown analytically that all the regular Bethe ansatz eigenstates of the 1D Hubbard model are the LWSs and the remaining eigenstates can be generated from the LWSs by applying  $\hat{\eta}^+$  [35–38].

Following them, we can construct the eigenstate having  $N_\eta$   $\eta$ -pairs from the LWS with  $N_\uparrow = N_\downarrow = N_0$  ( $\leq L/2$ ) as  $|\psi_{N_\eta}\rangle = \frac{1}{\sqrt{\mathcal{C}_{N_\eta}}} (\hat{\eta}^+)^{N_\eta} |\eta = \frac{L}{2} - N_0, \eta_z = -\eta\rangle$ , where the normalization constant is  $\mathcal{C}_{N_\eta} = N_\eta! \prod_{l=1}^{N_\eta} (L-2N_0-l+1)$  [39]. When  $|\psi_{N_\eta}\rangle$  is generated from the vacuum state

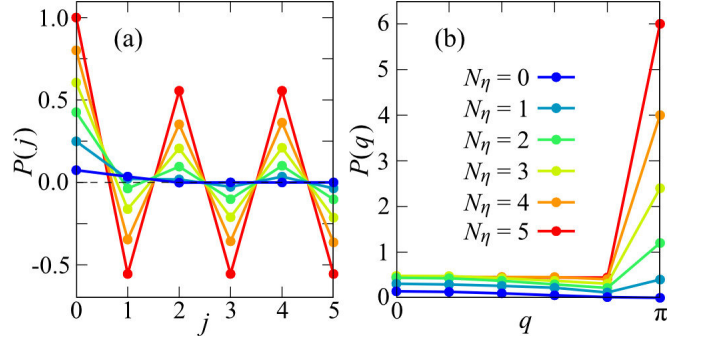


Figure 3. (a) On-site pair correlation function  $P(j)$  and (b) structure factor  $P(q)$  for the half-filled eigenstate  $|\psi_{N_\eta}\rangle$  at  $U = 8t_h$  with the different number of  $\eta$ -pairs  $N_\eta$  ( $\leq L/2$ ).  $|\psi_{N_\eta}\rangle$  is generated from the ground state  $|\psi_{N_0, N_0}^{(\text{GS})}\rangle$  of the Hubbard Hamiltonian  $\hat{\mathcal{H}}$  with  $N_0 = L/2 - N_\eta$  calculated by the ED for  $L = 10$  under PBC.

with  $N_0 = 0$ , it corresponds to Yang's  $\eta$ -pairing state  $|\phi_{N_\eta}\rangle$ . At half-filling,  $|\psi_{N_\eta}\rangle$  should contain  $L$  electrons and thus we consider  $|\psi_{N_\eta}\rangle$  with  $N_0 = L/2 - N_\eta$ . Therefore, in this case,  $|\psi_{N_\eta}\rangle \propto |\eta = N_\eta, \eta_z = 0\rangle$  and hence  $\langle \psi_{N_\eta} | \hat{\eta}^+ \hat{\eta}^- | \psi_{N_\eta} \rangle = N_\eta(N_\eta + 1)$ .

As an example, we construct  $|\psi_{N_\eta}\rangle$  from the ground state  $|\psi_{N_\uparrow, N_\downarrow}^{(\text{GS})}\rangle$  of  $\hat{\mathcal{H}}$  with  $N_\uparrow = N_\downarrow = N_0$  [40], which is the LWS. Figure 3 shows the on-site pair correlation,  $P(j)$  and  $P(q)$ , for  $|\psi_{N_\eta}\rangle$  with different  $N_\eta$  generated from  $|\psi_{N_0, N_0}^{(\text{GS})}\rangle$ . The sign alternating character in  $P(j)$  and the enhancement of  $P(q=\pi)$  are clearly observed. This is understood because  $P(q=\pi) = 2 \langle \psi_{N_\eta} | \hat{\eta}^+ \hat{\eta}^- | \psi_{N_\eta} \rangle / L = 2N_\eta(N_\eta + 1)/L$ . With increasing  $N_\eta$ ,  $|\psi_{N_\eta}\rangle$  crossovers to Yang's  $\eta$ -pairing state  $|\phi_{N_\eta=L/2}\rangle$  at  $N_\eta = L/2$ , for which  $P(q=\pi)$  is the largest.

To elucidate the nature of the photoinduced state  $|\Psi(t)\rangle$  in terms of the  $\eta$ -pairs, we calculate the eigenenergies  $\varepsilon_m$  and the structure factors  $P(q=\pi)$  for all the eigenstates  $|\psi_m\rangle$  of the Hubbard Hamiltonian  $\hat{\mathcal{H}}$  at half-filling. As shown in Fig. 4(a), the structure factor  $P(q=\pi)$  for each eigenstate is nicely quantized. This is because each eigenstate  $|\psi_m\rangle$  is also the eigenstate of  $\hat{\eta}^2$  and  $\hat{\eta}_z$ , and the quantized values are given as  $P(q=\pi) = 2 \langle \psi_m | \hat{\eta}^+ \hat{\eta}^- | \psi_m \rangle / L = 2\eta(\eta+1)/L$  with  $\eta = 0, 1, \dots, \frac{L}{2}$ , corresponding to the number of  $\eta$ -pairs [42].

In Fig. 4(a), color of each point indicates the weight  $|\langle \psi_m | \Psi(t) \rangle|^2$  of the eigenstate  $|\psi_m\rangle$  in the photoinduced state  $|\Psi(t)\rangle$  that exhibits the strong enhancement of  $P(q=\pi, t)$  after the pulse irradiation [see the inset of Fig 4(a)]. We find that the state  $|\Psi(t)\rangle$  after the pulse irradiation contains the non-zero weights of the eigenstates  $|\psi_m\rangle$  with finite  $\eta$  [also see Fig. 4(b)]. This is exactly the reason for the photoinduced enhancement of  $P(q=\pi, t)$ . The Hubbard model itself has the eigenstates with  $P(q=\pi) \neq 0$  and the photoinduced state  $|\Psi(t)\rangle$  captures the weights of those eigenstates.

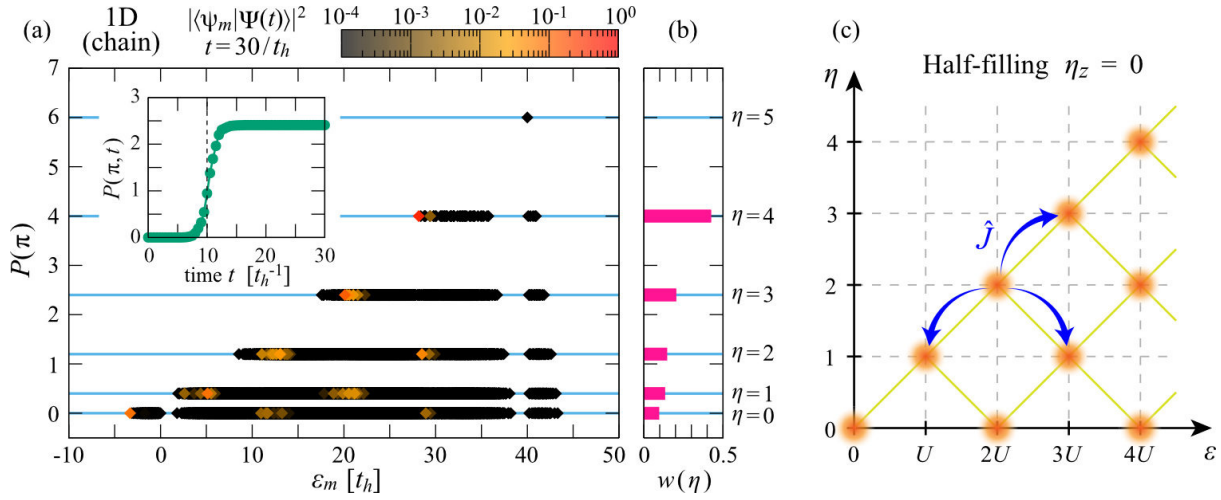


Figure 4. (a) All the eigenenergies  $\epsilon_m$  and  $P(q = \pi)$  for the eigenstates  $|\psi_m\rangle$  of the half-filled Hubbard Hamiltonian  $\hat{\mathcal{H}}$  at  $U = 8t_h$  and  $L = 10$  under PBC. Color of each point (diamond) indicates the weight  $|\langle \psi_m | \Psi(t) \rangle|^2$  of the eigenstate  $|\psi_m\rangle$  in the photoinduced state  $|\Psi(t)\rangle$  at  $t = 30/t_h$  for  $A(t)$  with  $A_0 = 0.4$ ,  $\omega_p = 7.8t_h$ ,  $\sigma_p = 2/t_h$ , and  $t_0 = 10/t_h$  [41]. The inset shows the time evolution of  $P(q = \pi, t)$  for  $|\Psi(t)\rangle$ . (b) Total weight  $w(\eta)$  of  $|\langle \psi_m | \Psi(t) \rangle|^2$  over the states  $|\psi_m\rangle$  with the same number  $\eta$  of  $\eta$ -pairs in (a). Note that  $\sum_{\eta=0}^{L/2} w(\eta) = 1$ . (c) Schematic figure of a ‘tower of states’  $|\psi_m\rangle$  in the photoinduced state  $|\Psi(t)\rangle$ . The initial state before the pulse irradiation is at  $(\epsilon, \eta) = (0, 0)$ . The current operator  $\hat{J}$  can induce the transition between states with  $\Delta\eta = \pm 1$  and  $\Delta\epsilon \sim \pm U$ , as indicated by arrows, assuming that  $\omega_p \sim U$ , and thus the pulse irradiation eventually excites a series of states with non-zero  $\eta$  and  $\epsilon$  (indicated by orange spheres).

The process of the enhancement of  $P(\pi, t)$  is explained as follows. Before the pulse irradiation, the initial state is the ground state of the Hubbard Hamiltonian  $\hat{\mathcal{H}}$  with  $|\eta = 0, \eta_z = 0\rangle$ , i.e., the  $\eta$  singlet state [38], and  $P(q = \pi) = 0$ . The pulse irradiation via  $A(t)$  breaks the commutation relation as  $[\hat{\mathcal{H}}(t), \hat{\eta}^\dagger] = [\hat{\mathcal{H}}, \hat{\eta}^\dagger] + \sum_k F(k, t) \hat{c}_{\pi-k, \downarrow}^\dagger \hat{c}_{k, \uparrow}^\dagger$  with  $F(k, t) = 4t_h \sin[A(t)] \sin k$ , and this transient breaking of the  $\eta$ -symmetry stirs states with different values of  $\eta$ . After the pulse irradiation, the Hamiltonian again satisfies the commutation relation because  $A(t) = 0$  but the state  $|\Psi(t)\rangle$  now contains components of  $|\eta \neq 0, \eta_z = 0\rangle$ , which enhance  $P(\pi, t)$ .

More precisely, in the small  $A_0$  limit, the external perturbation is expressed as  $A(t)\hat{J}$ , where  $\hat{J}$  is the current operator defined above. We can show that  $\hat{J}$  is a rank one tensor operator with the zero-th component in terms of the  $\hat{\eta}$ -operators [23]. Therefore, according to the Wigner-Eckart theorem for the tensor operators [43], there exists the selection rule such that  $\langle \eta', \eta'_z | \hat{J} | \eta, \eta_z \rangle \neq 0$  only for  $\eta' = \eta \pm 1$  when  $\eta'_z = \eta_z = 0$  at half-filling. This implies that in the linear response regime the photoinduced state  $|\Psi(t)\rangle$  can contain the eigenstates  $|\psi_m\rangle$  with  $\eta = 1$  and the eigenenergies  $\epsilon_m \sim U$ , assuming that  $\omega_p$  is tuned around  $U$ . This explains the good agreement between the optical spectrum  $\chi_{JJ}(\omega)$  and  $P(q = \pi, t)$  found in Fig. 2(b). At the second order, the photoinduced state  $|\Psi(t)\rangle$  can contain eigenstates  $|\psi_m\rangle$  of  $\hat{\mathcal{H}}$  with  $\eta = 2$  and  $\epsilon_m \sim 2U$ , as well as  $\eta = 0$  and  $\epsilon_m \sim 0$  and  $2U$ . Applying the same argument for higher orders,  $\eta$ -pairing eigenstates with even larger  $\eta$  values acquire in

the transient period a finite overlap  $|\langle \psi_m | \Psi(t) \rangle|^2$  with the photoinduced state. Considering all orders, eventually, the distribution of eigenstates  $|\psi_m\rangle$  in the photoinduced state forms a ‘tower of states’ shown schematically in Fig. 4(c), which is indeed in good qualitative accordance with the numerical results in Fig. 4(a) (also see Supplemental Material [23]). This also explains why the pulse irradiation is effective to induce  $\eta$ -pairs and the non-linearity is essential to enhance the pair correlation. Note that the non-linear response is absent in the non-interacting limit [i.e.,  $\chi_{JJ}(\omega) = 0$  for  $\omega \neq 0$ ], clearly showing the importance of electron correlations for the enhancement of superconductivity in this case.

Exactly the same argument can be applied to the two-dimensional Hubbard model on the square lattice and indeed we have found the large enhancement of the on-site pairing correlation in the photoinduced state, similar to the 1D case [23]. Although the enhancement of the pair correlation in the photoinduced state is most effective at half-filling, it remains even away from half-filling [23].

In conclusion, we have found that density-wave-like staggered superconducting correlations are induced by photo-exciting the MI ground state of the half-filled Hubbard model. The superconductivity is due to the  $\eta$ -pairing mechanism where the on-site singlet pairs display off-diagonal long range correlation with phase  $\pi$ , the fingerprint of the  $\eta$ -pairing state. We have shown that the non-linear optical response is essential to increase the number of  $\eta$ -pairs and hence enhance the superconducting correlation in a photo-excited state. The  $\eta$ -pairing states were originally introduced purely for the mathe-

mathematical purpose to solve the Hubbard model analytically, and here we have demonstrated that the pulse irradiation can bring this objects into the real world to be observed experimentally.

The authors acknowledge S. Sota, K. Seki, S. Miyakoshi, T. Oka, S. Kitamura, P. Werner, Y. Murakami, and S. Ishihara for fruitful discussion. This work was supported in part by Grants-in-Aid for Scientific Research from MEXT Japan under the Grant Nos.

17K05523, 18K13509, and 18H01183. The authors are grateful for providing computational resources of the K computer in RIKEN R-CCS through the HPCI System Research Project (Project Nos.: hp140130, hp150140, hp170324, and hp180098). The calculations were also performed in part on the RIKEN supercomputer system (HOKUSAI GreatWave) at Advanced Center for Computing and Communications (ACCC), RIKEN.

---

[1] Y. Tokura, *J. Phys. Soc. Jpn.* **75**, 011001 (2006).

[2] S. Iwai and H. Okamoto, *J. Phys. Soc. Jpn.* **75**, 011007 (2006).

[3] K. Yonemitsu and K. Nasu, *Phys. Rep.* **465**, 1 (2008).

[4] H. Aoki, N. Tsuji, M. Eckstein, M. Kollar, T. Oka, and P. Werner, *Rev. Mod. Phys.* **86**, 779 (2014).

[5] C. Giannetti, M. Capone, D. Fausti, M. Fabrizio, F. Parmigiani, and D. Mihailovic, *Adv. Phys.* **65**, 58 (2016).

[6] D. Fausti, R. I. Tobey, N. Dean, S. Kaiser, A. Dienst, M. C. Hoffmann, S. Pyon, T. Takayama, H. Takagi, and A. Cavalleri, *Science* **331**, 189 (2011).

[7] W. Hu, S. Kaiser, D. Nicoletti, C. R. Hunt, I. Gierz, M. C. Hoffmann, M. Le Tacon, T. Loew, B. Keimer, and A. Cavalleri, *Nat. Mater.* **13**, 705 (2014).

[8] S. Kaiser, C. R. Hunt, D. Nicoletti, W. Hu, I. Gierz, H. Y. Liu, M. Le Tacon, T. Loew, D. Haug, B. Keimer, and A. Cavalleri, *Phys. Rev. B* **89**, 184516 (2014).

[9] M. Mitrano, A. Cantaluppi, D. Nicoletti, S. Kaiser, A. Perucchi, S. Lupi, P. Di Pietro, D. Pontiroli, M. Riccò, S. R. Clark, D. Jaksch, and A. Cavalleri, *Nature (London)* **530**, 461 (2016).

[10] A. Cantaluppi, M. Buzzi, G. Jotzu, D. Nicoletti, M. Mitrano, D. Pontiroli, M. Riccò, A. Perucchi, P. Di Pietro, and A. Cavalleri, *Nat. Phys.* **14**, 837 (2018).

[11] M. A. Sentef, A. F. Kemper, A. Georges, and C. Kollath, *Phys. Rev. B* **93**, 144506 (2016).

[12] D. M. Kennes, E. Y. Wilner, D. R. Reichman, and A. J. Millis, *Nat. Phys.* **13**, 479 (2017).

[13] K. Ido, T. Ohgoe, and M. Imada, *Sci. Adv.* **3**, e1700718 (2017).

[14] G. Mazza and A. Georges, *Phys. Rev. B* **96**, 064515 (2017).

[15] S. Iwai, M. Ono, A. Maeda, H. Matsuzaki, H. Kishida, H. Okamoto, and Y. Tokura, *Phys. Rev. Lett.* **91**, 057401 (2003).

[16] H. Okamoto, H. Matsuzaki, T. Wakabayashi, Y. Takahashi, and T. Hasegawa, *Phys. Rev. Lett.* **98**, 037401 (2007).

[17] H. Uemura, H. Matsuzaki, Y. Takahashi, T. Hasegawa, and H. Okamoto, *J. Phys. Soc. Jpn.* **77**, 113714 (2008).

[18] H. Okamoto, T. Miyagoe, K. Kobayashi, H. Uemura, H. Nishioka, H. Matsuzaki, A. Sawa, and Y. Tokura, *Phys. Rev. B* **82**, 060513 (2010).

[19] H. Okamoto, T. Miyagoe, K. Kobayashi, H. Uemura, H. Nishioka, H. Matsuzaki, A. Sawa, and Y. Tokura, *Phys. Rev. B* **83**, 125102 (2011).

[20] T. Oka and H. Aoki, *Phys. Rev. B* **78**, 241104 (2008).

[21] T. Oka, *Phys. Rev. B* **86**, 075148 (2012).

[22] M. Eckstein and P. Werner, *Phys. Rev. Lett.* **110**, 126401 (2013).

[23] See Supplemental Material for details of numerical method, symmetry analysis, and time dependent perturbation analysis as well as the numerical results of larger chains and two dimensional case.

[24] R. Peierls, *Z. Phys.* **80**, 763 (1933).

[25] A. Takahashi, H. Itoh, and M. Aihara, *Phys. Rev. B* **77**, 205105 (2008).

[26] G. De Filippis, V. Cataudella, E. A. Nowadnick, T. P. Devereaux, A. S. Mishchenko, and N. Nagaosa, *Phys. Rev. Lett.* **109**, 176402 (2012).

[27] H. Lu, S. Sota, H. Matsueda, J. Bonča, and T. Tohyama, *Phys. Rev. Lett.* **109**, 197401 (2012).

[28] H. Hashimoto and S. Ishihara, *Phys. Rev. B* **93**, 165133 (2016).

[29] Y. Wang, M. Claassen, B. Moritz, and T. P. Devereaux, *Phys. Rev. B* **96**, 235142 (2017).

[30] M. Eckstein and P. Werner, *Phys. Rev. B* **84**, 035122 (2011).

[31] P. Werner, K. Held, and M. Eckstein, *Phys. Rev. B* **90**, 235102 (2014).

[32] H. Yanagiya, Y. Tanaka, and K. Yonemitsu, *J. Phys. Soc. Jpn.* **84**, 094705 (2015).

[33] The spin structure factor is defined as  $S(q, t) = \sum_j e^{iqR_j} S(j, t)$  with  $S(j, t) = \frac{1}{L} \sum_i \langle \Psi(t) | \hat{m}_{i+j}^z \hat{m}_i^z | \Psi(t) \rangle$  and  $\hat{m}_i^z = \hat{n}_{i,\uparrow} - \hat{n}_{i,\downarrow}$ .

[34] C. N. Yang, *Phys. Rev. Lett.* **63**, 2144 (1989).

[35] Same for the spin sector.

[36] F. H. L. Essler, V. E. Korepin, and K. Schoutens, *Phys. Rev. Lett.* **67**, 3848 (1991).

[37] F. H. Essler, V. E. Korepin, and K. Schoutens, *Nucl. Phys. B* **372**, 559 (1992).

[38] F. H. Essler, H. Frahm, F. Göhmann, A. Klümper, and V. E. Korepin, *The One-Dimensional Hubbard Model* (Cambridge University Press, Cambridge, 2005).

[39] M. Takahashi, *Thermodynamics of One Dimensional Solvable Models* (Cambridge University Press, Cambridge, 1999).

[40] Note that the state  $|\psi_{N_\eta}\rangle$  is the exact eigenstate of  $\hat{H}$  with the eigenenergy  $E_{N_0} + N_\eta U$  ( $< LU/2$ ), where  $E_{N_0}$  ( $< N_0 U$ ) is the eigenenergy of  $|\psi_{N_0, N_0}^{(GS)}\rangle$ .

[41] When the eigenstates  $|\psi_m\rangle$  are degenerate, the sum of  $|\langle \psi_m | \Psi(t) \rangle|^2$  over these degenerate states is indicated.

[42] These quantized values are exactly the same as  $P(q = \pi)$  calculated for  $|\psi_{N_\eta}\rangle$  shown in Fig. 3(b).

[43] J. J. Sakurai, *Modern Quantum Mechanics* (Addison Wesley, 1993); M. E. Rose, *Elementary Theory of Angular Momentum* (Wiley, New York, 1967)

## SUPPLEMENTAL MATERIAL

### 1. Exact diagonalization method

To evaluate the state  $|\Psi(t)\rangle$  under the time-dependent Hamiltonian  $\hat{\mathcal{H}}(t)$ , we numerically solve the time-dependent Schrödinger equation,

$$i \frac{\partial}{\partial t} |\Psi(t)\rangle = \hat{\mathcal{H}}(t) |\Psi(t)\rangle, \quad (\text{S1})$$

with the initial condition that  $|\Psi(t=0)\rangle = |\psi_0\rangle$ , where  $|\psi_0\rangle$  is the ground state of the Hamiltonian  $\hat{\mathcal{H}}(t=0)$ . For this purpose, we employ the time-dependent exact diagonalization (ED) method based on the Lanczos algorithm [S1, S2]. In this method, the time evolution with a short time step  $\delta t$  is calculated as

$$\begin{aligned} |\Psi(t + \delta t)\rangle &\simeq e^{-i\hat{\mathcal{H}}(t)\delta t} |\Psi(t)\rangle \\ &\simeq \sum_{\ell=1}^{M_L} e^{-i\xi_\ell \delta t} |\tilde{\psi}_\ell\rangle \langle \tilde{\psi}_\ell | \Psi(t) \rangle, \end{aligned} \quad (\text{S2})$$

where  $\xi_\ell$  and  $|\tilde{\psi}_\ell\rangle$  are eigenenergies and eigenvectors of  $\hat{\mathcal{H}}(t)$ , respectively, in the corresponding Krylov subspace generated with  $M_L$  Lanczos iterations [S1–S3]. In our ED calculations, we adopt  $\delta t = 0.01/t_h$  and  $M_L = 15$  for the time evolution, which provides results with almost machine precision accuracy.

### 2. One-dimensional (1D) Hubbard model with larger $L$ : a MPS study

#### Method

In order to confirm the enhancement of the pair correlation in larger systems, we also perform the time-dependent matrix-product state (MPS) [S4] simulation for the time evolution starting from the ground state of the Hubbard Hamiltonian  $\hat{\mathcal{H}}$  calculated by the density-matrix renormalization group method [S5, S6]. For the time evolution simulation, we employ the method proposed in Ref. [S7], in which the time evolution operator is factorized as a compact form of the matrix product operator (MPO) representation. In this method, the higher order approximation for the time evolution operator with time step  $\delta t$  are formulated by introducing the additional set of time steps  $\{\delta t_1, \delta t_2, \dots, \delta t_n\}$  with complex numbers in order to eliminate the unnecessary lowest order terms arisen from the MPO factorization. The resulting error is  $\mathcal{O}(L\delta t^p)$ , where  $L$  and  $p$  denote the system size and the order of the approximation, respectively. Our calculation sets  $p = 3$ , which requires the additional  $n = 4$  time steps, i.e.,  $\delta t_1 = a + ib$ ,  $\delta t_2 = a - ib$ ,  $\delta t_3 = b + ia$ , and  $\delta t_4 = b - ia$ , with  $a = (3 + \sqrt{3})/12$  and  $b = (3 - \sqrt{3})/12$ .

For the MPS simulation, we use the ITensor package [S8]. We keep the bond dimension up to  $m = 1200$  to

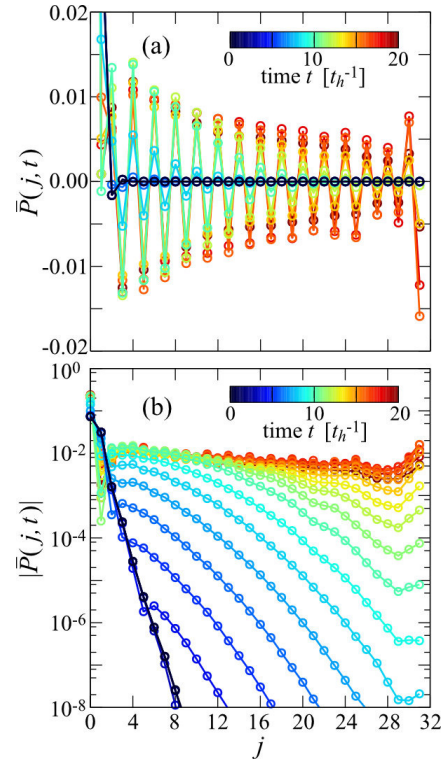


Figure S.1. Time-dependence of the on-site pair correlation function (a)  $\bar{P}(j, t)$  and (b) logarithm of  $|\bar{P}(j, t)|$  calculated by the time-dependent MPS method for a chain of  $L = 32$  sites with OBC at  $U = 8t_h$ . Here,  $A_0 = 0.2$ ,  $\omega_p = 8.26t_h$ ,  $\sigma_p = 2/t_h$ , and  $t_0 = 8/t_h$  are adopted in the vector potential  $A(t)$ .

calculate the ground state of  $\hat{\mathcal{H}}$  for the initial state and  $m = 4800$  for the time evolution of the  $L = 32$  system under open boundary conditions (OBC). The time step  $\delta t$  is set to be  $\delta t = 0.01/t_h$ .

#### Results

Figure S.1 shows the real-space on-site pair correlation function

$$\bar{P}(j, t) = \frac{1}{N_b} \sum_{i=1}^{N_b} \langle \Psi(t) | (\hat{\Delta}_{i+j}^\dagger \hat{\Delta}_i + \text{H.c.}) | \Psi(t) \rangle, \quad (\text{S3})$$

where  $\hat{\Delta}_i = \hat{c}_{i,\uparrow} \hat{c}_{i,\downarrow}$  and  $N_b = L - j$  is the number of pairs of sites separated by distance  $j$  in the system of  $L$  sites with OBC. As shown in Fig. S.1, the pair correlation extends to a longer distance gradually with time in the transient period and shows clearly the sign alternating feature that is characteristic of the  $\eta$ -pairing. The pair correlation eventually reaches to the longest distance in the system, similar to the results shown in Figs. 1(a) and 1(b) in the main text.

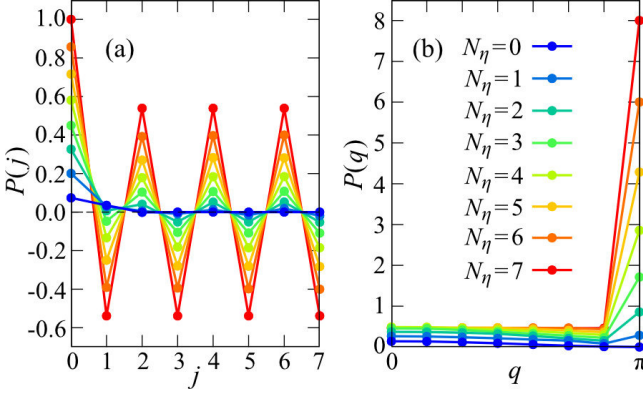


Figure S.2. (a) On-site pair correlation function  $P(j)$  and (b) on-site pair structure factor  $P(q)$  for the half-filled eigenstate  $|\psi_{N_\eta}\rangle$  at  $U = 8t_h$  with the different number of  $\eta$ -pairs  $N_\eta$  ( $\leq L/2$ ).  $|\psi_{N_\eta}\rangle$  is generated from the ground state  $|\psi_{N_0, N_0}^{(\text{GS})}\rangle$  of the Hubbard Hamiltonian  $\hat{\mathcal{H}}$  with  $N_0 = L/2 - N_\eta$  calculated by the ED method for  $L = 14$  under PBC.

### 3. $\eta$ -pairing in the 1D Hubbard model for $L = 14$

As an example, Fig. 3 in the main text shows the on-site pair correlation  $P(j)$  and  $P(q)$  of the  $\eta$ -pairing eigenstate

$$|\psi_{N_\eta}\rangle = \frac{1}{\sqrt{\mathcal{C}_{N_\eta}}} (\hat{\eta}^+)^{N_\eta} |\psi_{N_0, N_0}^{(\text{GS})}\rangle \quad (\text{S4})$$

for  $L = 10$  simply because of the correspondence to Fig. 4(a) calculated for the 10 site cluster. Here, we show supplementarily the results of  $P(j)$  and  $P(q)$  for  $L = 14$  at half-filling in Fig. S.2. The ground state  $|\psi_{N_0, N_0}^{(\text{GS})}\rangle$  of the Hubbard Hamiltonian  $\hat{\mathcal{H}}$  with  $N_\uparrow = N_\downarrow = N_0 = L/2 - N_\eta$  is calculated by the ED method under periodic boundary conditions (PBC). Note that  $|\psi_{N_\eta}\rangle$  is the eigenstate of  $\hat{\mathcal{H}}$  at half-filling with  $N_\eta$   $\eta$ -pairs. As shown in Fig. S.2, the density-wave-like pair correlation is largest for  $N_\eta = L/2$ .

### 4. Hubbard model on the square lattice

In the main text, we focus on the 1D Hubbard model to demonstrate that the strong superconducting correlation can be induced in the Mott insulator (MI) by the pulse irradiation, and we show that the origin of this superconductivity is due to the  $\eta$ -pairing mechanism. Here, we show that exactly the same conclusion can be reached for the two-dimensional (2D) Hubbard model on the square lattice with only nearest neighbor hoppings.

### Model and $\eta$ -operators

The 2D Hubbard model is described by the following Hamiltonian:

$$\hat{\mathcal{H}} = -t_h \sum_{\langle i, j \rangle} \sum_{\sigma} \left( \hat{c}_{i,\sigma}^\dagger \hat{c}_{j,\sigma} + \text{H.c.} \right) + U \sum_i \hat{n}_{i,\uparrow} \hat{n}_{i,\downarrow}, \quad (\text{S5})$$

where the sum  $\langle i, j \rangle$  runs over all pairs of nearest neighbor sites  $i$  and  $j$  on the square lattice. Similarly to the 1D case, the total  $\hat{\eta}$ -operators  $\hat{\eta}^\pm = \sum_j \hat{\eta}_j^\pm$  and  $\hat{\eta}_z = \sum_j \hat{\eta}_j^z$  are defined in terms of the local operators  $\hat{\eta}_j^+ = (-1)^{j_x+j_y} \hat{c}_{j,\downarrow}^\dagger \hat{c}_{j,\uparrow}^\dagger$ ,  $\hat{\eta}_j^- = (-1)^{j_x+j_y} \hat{c}_{j,\uparrow} \hat{c}_{j,\downarrow}$ , and  $\hat{\eta}_j^z = \frac{1}{2} (\hat{n}_{j,\uparrow} + \hat{n}_{j,\downarrow} - 1)$ , where the location of site  $j$  is given as  $\mathbf{R}_j = j_x \mathbf{e}_x + j_y \mathbf{e}_y$  and  $\mathbf{e}_{x(y)}$  is the unit vector along the  $x(y)$  direction. These operators satisfy the  $SU(2)$  commutation relations. We can also show that  $[\hat{\mathcal{H}}, \hat{\eta}^\pm] = \pm U \hat{\eta}^\pm$  and  $[\hat{\mathcal{H}}, \hat{\eta}^+ \hat{\eta}^-] = [\hat{\mathcal{H}}, \hat{\eta}_z] = 0$ . Therefore, any eigenstate of the Hubbard Hamiltonian  $\hat{\mathcal{H}}$  can be chosen also to be an eigenstate  $|\eta, \eta_z\rangle$  of  $\hat{\eta}^2 = \frac{1}{2} (\hat{\eta}^+ \hat{\eta}^- + \hat{\eta}^- \hat{\eta}^+) + \hat{\eta}_z^2$  and  $\hat{\eta}_z$  with the eigenvalues  $\eta(\eta+1)$  and  $\eta_z$ , respectively, where  $|\eta, \eta_z\rangle$  can take  $\eta = 0, 1, 2, \dots, L/2$  and  $\eta_z = -\eta, -\eta+1, \dots, \eta$ , assuming that the number  $N_\uparrow$  of up electrons and the number  $N_\downarrow$  of down electrons are the same and  $L$  (even) is the total number of sites. At half-filling with  $N_\uparrow = N_\downarrow = L/2$ , the eigenstates are characterized with  $\eta = 0, 1, 2, \dots, L/2$  and  $\eta_z = 0$ , and the ground state  $|\psi_0\rangle$  of the Hubbard Hamiltonian  $\hat{\mathcal{H}}$  is  $\eta = \eta_z = 0$ .

The real-space on-site pair correlation function for the time-evolved state  $|\Psi(t)\rangle$  is defined as

$$P(\mathbf{R}_j, t) = \frac{1}{L} \sum_i \langle \Psi(t) | \left( \hat{\Delta}_{\mathbf{R}_i + \mathbf{R}_j}^\dagger \hat{\Delta}_{\mathbf{R}_i} + \text{H.c.} \right) | \Psi(t) \rangle, \quad (\text{S6})$$

where  $\hat{\Delta}_{\mathbf{R}_i} = \hat{c}_{i,\uparrow} \hat{c}_{i,\downarrow}$  and the pair structure factor in the momentum space is given as

$$P(\mathbf{q}, t) = \sum_j e^{i\mathbf{q} \cdot \mathbf{R}_j} P(\mathbf{R}_j, t). \quad (\text{S7})$$

Noticing that  $\hat{\Delta}_{\mathbf{R}_j} = (-1)^{j_x+j_y} \hat{\eta}_j^-$ ,  $P(\mathbf{q}, t)$  at  $\mathbf{q} = \mathbf{\pi} = (\pi, \pi)$  is

$$P(\mathbf{q} = \mathbf{\pi}, t) = \frac{2}{L} \langle \Psi(t) | \hat{\eta}^+ \hat{\eta}^- | \Psi(t) \rangle \quad (\text{S8})$$

$$= \frac{2}{L} \langle \Psi(t) | (\hat{\eta}^2 - \hat{\eta}_z^2 + \hat{\eta}_z) | \Psi(t) \rangle. \quad (\text{S9})$$

The pair structure factor  $P(\mathbf{q} = \mathbf{\pi})$  for  $|\eta, \eta_z\rangle$  is thus  $2[\eta(\eta+1) - \eta_z(\eta_z-1)]/L$ .

Any eigenstate  $|\eta, \eta_z\rangle$  can be constructed from the LWS  $|\eta, -\eta\rangle$  by repeatedly applying  $\hat{\eta}^+$  because

$$\hat{\eta}^+ |\eta, \eta_z\rangle = \sqrt{\eta(\eta+1) - \eta_z(\eta_z+1)} |\eta, \eta_z+1\rangle. \quad (\text{S10})$$

Since  $\hat{\eta}^- |\eta, -\eta\rangle = 0$  by definition, the LWS contains no  $\eta$ -pairs and  $P(\mathbf{q} = \mathbf{\pi}) = 0$ . Each time that  $\hat{\eta}^+$  is applied from the LWS, the number of  $\eta$ -pairs increases by

one, and the maximum number of  $\eta$ -pairs is obtained when  $\eta_z = 0$  (i.e., half-filling) for a given  $\eta$ , where  $\langle \eta, \eta_z = 0 | \hat{\eta}^+ \hat{\eta}^- | \eta, \eta_z = 0 \rangle = \eta(\eta + 1)$  and the number of  $\eta$ -pairs is  $\eta$ .

The time-dependent external field is introduced in Eq. (S5) by  $t_h \hat{c}_{i,\sigma}^\dagger \hat{c}_{j,\sigma} \rightarrow t_h e^{-i\mathbf{A}(t) \cdot (\mathbf{R}_i - \mathbf{R}_j)} \hat{c}_{i,\sigma}^\dagger \hat{c}_{j,\sigma}$  with the time-dependent vector potential  $\mathbf{A}(t) = A(t)(\mathbf{e}_x + \mathbf{e}_y)$  pointing along the diagonal direction and  $A(t)$  given in the main text. The current operator  $\hat{J}_\alpha^{(0)}$  along a direction  $\alpha$  ( $\alpha = x, y$ ) is defined as

$$\hat{J}_\alpha^{(0)} = it_h \sum_{j,\sigma} \left( \hat{c}_{j+\mathbf{e}_\alpha,\sigma}^\dagger \hat{c}_{j,\sigma} - \hat{c}_{j,\sigma}^\dagger \hat{c}_{j+\mathbf{e}_\alpha,\sigma} \right), \quad (\text{S11})$$

where  $\hat{c}_{j+\mathbf{e}_\alpha,\sigma}^\dagger$  is the creation operator of an electron at the site located at  $\mathbf{R}_j + \mathbf{e}_\alpha$  with spin  $\sigma$ . We can now show that

$$[\hat{\eta}^\pm, \hat{J}_\alpha^{(0)}] = \sqrt{2} \hat{J}_\alpha^{(\pm 1)}, \quad [\hat{\eta}_z, \hat{J}_\alpha^{(0)}] = 0, \quad (\text{S12})$$

$$[\hat{\eta}^\pm, \hat{J}_\alpha^{(\mp 1)}] = \sqrt{2} \hat{J}_\alpha^{(0)}, \quad [\hat{\eta}_z, \hat{J}_\alpha^{(\pm 1)}] = \pm \hat{J}_\alpha^{(\pm 1)}, \quad (\text{S13})$$

where

$$\hat{J}_\alpha^{(+1)} = \sqrt{2} it_h \sum_j (-1)^{j_x + j_y} (\hat{c}_{j+\mathbf{e}_\alpha,\uparrow}^\dagger \hat{c}_{j,\downarrow}^\dagger + \hat{c}_{j,\uparrow}^\dagger \hat{c}_{j+\mathbf{e}_\alpha,\downarrow}^\dagger), \quad (\text{S14})$$

and

$$\hat{J}_\alpha^{(-1)} = \sqrt{2} it_h \sum_j (-1)^{j_x + j_y} (\hat{c}_{j+\mathbf{e}_\alpha,\downarrow}^\dagger \hat{c}_{j,\uparrow}^\dagger + \hat{c}_{j,\downarrow}^\dagger \hat{c}_{j+\mathbf{e}_\alpha,\uparrow}^\dagger). \quad (\text{S15})$$

Therefore,  $\hat{J}_\alpha^{(q)}$  with  $q = 0, \pm 1$  is a rank one tensor operator in terms of  $\hat{\eta}$ -operators. In particular, the current operator  $\hat{J}_\alpha^{(0)}$  is a rank one tensor operator with  $q = 0$  and hence there is the following selection rule:  $\langle \eta', \eta'_z | \hat{J}_\alpha^{(0)} | \eta, \eta_z \rangle \neq 0$  only for  $\eta' = \eta \pm 1$  when  $\eta'_z = \eta_z = 0$  [S9, S10]. We also note that  $it_h \sum_{\langle i,j \rangle} \sum_\sigma \sin [\mathbf{A}(t) \cdot (\mathbf{R}_i - \mathbf{R}_j)] (\hat{c}_{i,\sigma}^\dagger \hat{c}_{j,\sigma} - \text{H.c.})$  is a rank one tensor operator with  $q = 0$ , while  $-t_h \sum_{\langle i,j \rangle} \sum_\sigma \cos [\mathbf{A}(t) \cdot (\mathbf{R}_i - \mathbf{R}_j)] (\hat{c}_{i,\sigma}^\dagger \hat{c}_{j,\sigma} + \text{H.c.})$  is a rank zero tensor operator, i.e., a scalar operator.

Although here we consider the 2D case, the extension to other spatial dimensions is straightforward.

### Results

As shown above, any eigenstate of  $\hat{\mathcal{H}}$  can be chosen to be an eigenstate of  $\hat{\eta}^2$  and  $\hat{\eta}_z$ . Figure S.3(a) shows all the eigenenergies  $\varepsilon_m$  of  $\hat{\mathcal{H}}$  and the corresponding pair structure factors  $P(\mathbf{q})$  at  $\mathbf{q} = \mathbf{\pi} = (\pi, \pi)$  on a  $\sqrt{10} \times \sqrt{10}$  cluster with PBC at half-filling. Indeed, as in the 1D case,  $P(\mathbf{\pi})$  is quantized as  $P(\mathbf{\pi}) = 2\eta(\eta + 1)/L$ , where  $\eta (= 0, 1, \dots, L/2)$  corresponds to the number of  $\eta$ -pairs.

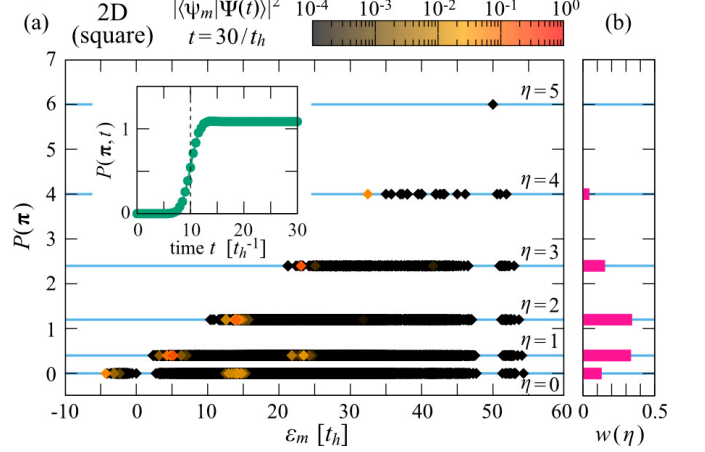


Figure S.3. (a) All the eigenenergies  $\varepsilon_m$  and  $P(\mathbf{q} = \mathbf{\pi})$  [ $\mathbf{\pi} = (\pi, \pi)$ ] for the eigenstates  $|\psi_m\rangle$  of the half-filled Hubbard model on a  $\sqrt{10} \times \sqrt{10}$  cluster with PBC at  $U = 10t_h$ . Color of each point (diamond) indicates the weight  $|\langle \psi_m | \Psi(t) \rangle|^2$  of the eigenstate  $|\psi_m\rangle$  in the photoinduced state  $|\Psi(t)\rangle$  at  $t = 30/t_h$ . Here,  $A_0 = 0.25$ ,  $\omega_p = 9.1t_h$ ,  $\sigma_p = 2/t_h$ , and  $t_0 = 10/t_h$  are adopted in the vector potential  $A(t)$ . When the eigenstates are degenerated, color indicates the sum of  $|\langle \psi_m | \Psi(t) \rangle|^2$  over these degenerate states. The time evolution of  $P(\mathbf{q} = \mathbf{\pi}, t)$  for  $|\Psi(t)\rangle$  is also shown in the inset. (b) Total weight  $w(\eta)$  of  $|\langle \psi_m | \Psi(t) \rangle|^2$  over the states  $|\psi_m\rangle$  that have the same number  $\eta$  of  $\eta$ -pairs, and thus  $\sum_{\eta=0}^{L/2} w(\eta) = 1$ . The parameters are the same as in (a).

As shown in Fig S.3(b), the photoinduced state  $|\Psi(t)\rangle$  after the pulse irradiation displays non-zero overlaps with the eigenstates  $|\psi_m\rangle$  of  $\hat{\mathcal{H}}$  with  $\eta \neq 0$ . This is responsible for the large enhancement of  $P(\mathbf{q}, t)$  in the photoinduced state  $|\Psi(t)\rangle$  [see the inset of Fig. S.3(a)]. Since the current operator is a rank one tensor operator, we can again observe in Fig. S.3(a) a “tower of states” structure of the eigenstates  $|\psi_m\rangle$  contributing to the photoinduced state  $|\Psi(t)\rangle$  with large weights  $|\langle \psi_m | \Psi(t) \rangle|^2$ .

### 5. 1D Hubbard model away from half-filling

We also examine the behavior of the photoinduced states in the 1D Hubbard model  $\hat{\mathcal{H}}$  away from half-filling. Figure S.4 shows the time evolution of the pair correlation function  $P(j, t)$  calculated by the ED method for  $L = 12$  with  $N_\uparrow = N_\downarrow = 5$  (10 electrons in total) under PBC. Although the magnitude of  $P(j, t)$  is smaller than that for the case of half-filling,  $P(j, t)$  clearly shows a pair density wave like oscillation with the correlation extended up to the longest distance of the cluster. Therefore, the  $\eta$ -pairing correlation is induced in the photo-excited state in the Hubbard model even away from half-filling.

To elucidate the nature of the photoinduced state  $|\Psi(t)\rangle$  in terms of the  $\eta$ -pairs, we calculate the eigenen-

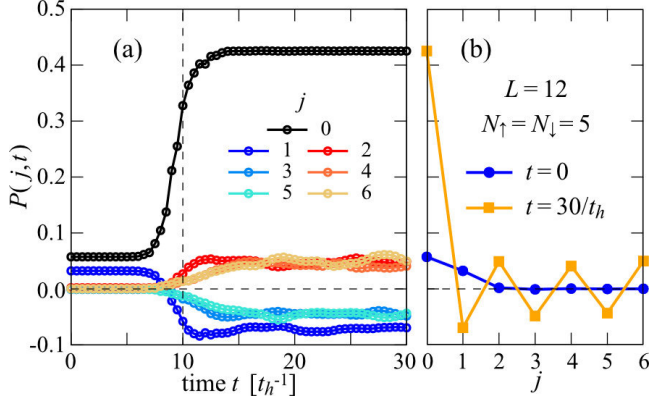


Figure S.4. (a) Time evolution of the on-site pair correlation function  $P(j,t)$  with hole doping. (b)  $P(j,t)$  at  $t = 0$  (blue circles) and  $t = 30/t_h$  (orange squares). The results are calculated by the ED method for  $L = 12$  and  $N_\uparrow = N_\downarrow = 5$  at  $U = 8t_h$  with  $\sigma_p = 2/t_h$ ,  $t_0 = 10/t_h$ ,  $A_0 = 0.7$ , and  $\omega_p = 8.8t_h$ .

ergies  $\varepsilon_m$  and the structure factors  $P(q=\pi)$  for all the eigenstates  $|\psi_m\rangle$  of the 1D Hubbard Hamiltonian  $\hat{\mathcal{H}}$  with hole-doping. Figure S.5 shows the results for  $L = 8$  with  $N_\uparrow = N_\downarrow = 3$  (6 electrons in total) under PBC. As shown in Fig. S.5(a), the structure factor  $P(q=\pi)$  for each eigenstate is nicely quantized. This is because each eigenstate  $|\psi_m\rangle$  away from half-filling is also the eigenstate of  $\hat{\eta}^2$  and  $\hat{\eta}_z$ . The quantized values are given as

$$\begin{aligned} P(\pi) &= \frac{2}{L} \langle \psi_m | \hat{\eta}^+ \hat{\eta}^- | \psi_m \rangle = \frac{2}{L} \langle \psi_m | (\hat{\eta}^2 - \hat{\eta}_z^2 + \hat{\eta}_z) | \psi_m \rangle \\ &= \frac{2}{L} [\eta(\eta+1) - \eta_z(\eta_z-1)] \end{aligned} \quad (\text{S16})$$

with  $\eta = |\eta_z|$ ,  $|\eta_z|+1, \dots, \frac{L}{2}$  and  $\eta_z = (N_\uparrow + N_\downarrow - L)/2 = -1$ . Note that  $P(\pi) = 0$  (no  $\eta$ -pair state) is characterized by the state with  $\eta = 1$  because  $\eta_z = -1$  and this state is the LWS.

In Fig. S.5(a), color of each point indicates the weight  $|\langle \psi_m | \Psi(t) \rangle|^2$  of the eigenstate  $|\psi_m\rangle$  in the photoinduced state  $|\Psi(t)\rangle$  that exhibits the enhancement of  $P(q=\pi, t)$  after the pulse irradiation [see the inset of Fig S.5(a)]. We find that the state  $|\Psi(t)\rangle$  after the pulse irradiation contains the non-zero weights of the eigenstates  $|\psi_m\rangle$  with finite  $P(\pi)$  [also see Fig. S.5(b)]. Therefore, the reason for the enhancement of  $P(q=\pi, t)$  is the same as in the case at half-filling.

However, the distribution of the weight  $|\langle \psi_m | \Psi(t) \rangle|^2$  after the pulse irradiation in Fig. S.5(a) is qualitatively different from that in the case at half-filling shown in Fig. 4(a) in the main text. For example, there is the finite contribution to the weight from the eigenstates with  $P(\pi) = 0$  around  $\varepsilon_m - \varepsilon_0 \sim \omega_p$ , which is absent at half-filling. This is explained by the different selection rules of the current operator  $\hat{J}$  for the half-filled ( $\eta_z = 0$ ) and hole-doped ( $\eta_z \neq 0$ ) states. As mentioned in the main text and also in Sec. 4,  $\hat{J}$  is a rank one tensor operator

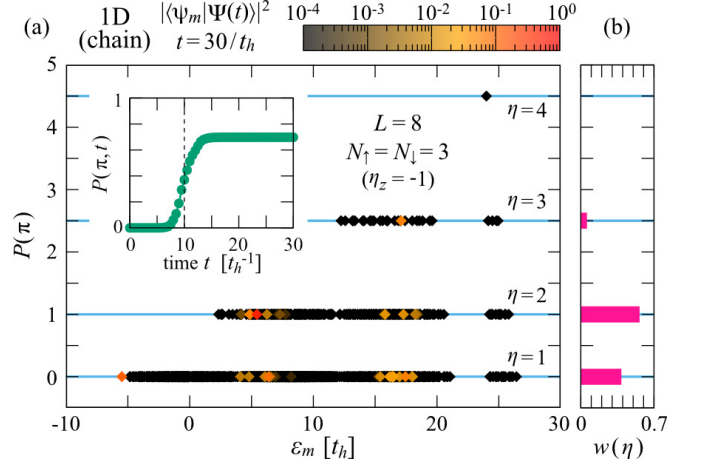


Figure S.5. (a) All the eigenenergies  $\varepsilon_m$  and  $P(q = \pi)$  for the eigenstates  $|\psi_m\rangle$  of the hole-doped 1D Hubbard Hamiltonian  $\hat{\mathcal{H}}$  at  $U = 8t_h$  for  $L = 8$  under PBC with  $N_\uparrow = N_\downarrow = 3$  electrons. Color of each point (diamond) indicates the weight  $|\langle \psi_m | \Psi(t) \rangle|^2$  of the eigenstate  $|\psi_m\rangle$  in the photoinduced state  $|\Psi(t)\rangle$  at  $t = 30/t_h$ . Here,  $A_0 = 0.7$ ,  $\omega_p = 10.7t_h$ ,  $\sigma_p = 2/t_h$ , and  $t_0 = 10/t_h$  are adopted in the vector potential  $A(t)$ . When the eigenstates are degenerated, color indicates the sum of  $|\langle \psi_m | \Psi(t) \rangle|^2$  over these degenerate states. The time evolution of  $P(q = \pi, t)$  for  $|\Psi(t)\rangle$  is also shown in the inset. (b) Total weight  $w(\eta)$  of  $|\langle \psi_m | \Psi(t) \rangle|^2$  over the states  $|\psi_m\rangle$  that have the same eigenvalue of  $\hat{\eta}$ , and thus  $\sum_{\eta=1}^{L/2} w(\eta) = 1$ . The parameters are the same as in (a). Note that the number of  $\eta$ -pairs is  $\eta - 1$  for this hole-doped case.

with the zero-th component in terms of the  $\hat{\eta}$ -operators. Hence, from the Wigner–Eckart theorem [S9, S10], the selection rule of  $\langle \eta', \eta'_z | \hat{J} | \eta, \eta_z \rangle$  is given as

$$\langle \eta', \eta'_z | \hat{J} | \eta, \eta_z \rangle \propto \begin{pmatrix} \eta & 1 & \eta' \\ \eta_z & 0 & -\eta'_z \end{pmatrix} \quad (\text{S17})$$

with the  $3j$ -symbol. The  $3j$ -symbol is zero unless  $\eta - 1 \leq \eta' \leq \eta + 1$  and  $\eta_z - \eta'_z = 0$  are satisfied. Therefore,  $\langle \eta', \eta'_z | \hat{J} | \eta, \eta_z \rangle \neq 0$  for  $\eta' = \eta$ ,  $\eta \pm 1$  when  $\eta'_z = \eta_z \neq 0$  for the hole-doped states. The result in Fig. S.5(a) follows this selection rule. However, when  $\eta_z = \eta'_z = 0$  for the half-filled state, the nonzero  $3j$ -symbol must satisfy the additional rule:  $\eta + \eta' + 1 = (\text{even})$ . Therefore, the excitation to the states with  $\eta' = \eta$  is not induced by  $\hat{J}$  at half-filling ( $\eta_z = \eta'_z = 0$ ), and  $\langle \eta', 0 | \hat{J} | \eta, 0 \rangle \neq 0$  only for  $\eta' = \eta \pm 1$ . The results at half-filling in Fig. 4(a) in the main text and Fig. S.3(a) follow this selection rule.

## 6. Perturbation analysis in the limit of large pulse width $\sigma_p$

In the large pulse width limit, i.e.,  $\sigma_p \rightarrow \infty$ , the time-dependent vector potential is given as  $A(t) = A_0 \cos[\omega_p(t - t_0)]$ . Let us denote the time-dependent

Hamiltonian with the time-dependent external field as

$$\hat{\mathcal{H}}(t) = \hat{\mathcal{H}} + \hat{\mathcal{V}}(t), \quad (\text{S18})$$

where  $\hat{\mathcal{H}}$  is the time-independent part of the Hamiltonian given by, e.g., Eq. (1) in the main text and  $\hat{\mathcal{V}}(t)$  is the time-dependent part of the Hamiltonian given as

$$\hat{\mathcal{V}}(t) = -t_h \sum_{j,\sigma} \left( e^{iA(t)} - 1 \right) \hat{c}_{j,\sigma}^\dagger \hat{c}_{j+1,\sigma} + \text{H.c..} \quad (\text{S19})$$

Because  $A(t)$  becomes a periodic function of  $t$  in the limit  $\sigma_p \rightarrow \infty$ ,  $\hat{\mathcal{V}}(t)$  can be expanded using Bessel functions of the first kind  $\mathcal{J}_\mu(x)$  ( $\mu$ : integer) [S11], i.e.,

$$\hat{\mathcal{V}}(t) = \sum_{\mu=-\infty}^{\infty} \hat{\mathcal{V}}^{(\mu)} e^{-i\mu\omega_p t}, \quad (\text{S20})$$

where

$$\begin{aligned} \hat{\mathcal{V}}^{(0)} &= (\mathcal{J}_0(A_0) - 1)\hat{K}, \\ \hat{\mathcal{V}}^{(2\mu)} &= (-1)^\mu \mathcal{J}_{2\mu}(A_0)\hat{K}, \quad (\mu \neq 0) \\ \hat{\mathcal{V}}^{(2\mu+1)} &= (-1)^\mu \mathcal{J}_{2\mu+1}(A_0)\hat{J}. \end{aligned} \quad (\text{S21})$$

Here we set  $t_0 = 0$ . It is important to notice in Eqs. (S20) and (S21) that the operator  $\hat{K}$  in the  $\mu$  even terms is the

kinetic (rank zero tensor) operator, i.e.,

$$\hat{K} = -t_h \sum_{j,\sigma} \left( \hat{c}_{j,\sigma}^\dagger \hat{c}_{j+1,\sigma} + \hat{c}_{j+1,\sigma}^\dagger \hat{c}_{j,\sigma} \right), \quad (\text{S22})$$

while the operator  $\hat{J}$  in the  $\mu$  odd terms is the current (rank one tensor) operator, i.e.,

$$\hat{J} = -it_h \sum_{j,\sigma} \left( \hat{c}_{j,\sigma}^\dagger \hat{c}_{j+1,\sigma} - \hat{c}_{j+1,\sigma}^\dagger \hat{c}_{j,\sigma} \right), \quad (\text{S23})$$

as defined also in the main text.

A time-dependent state  $|\Psi(t)\rangle$  governed by  $\hat{\mathcal{H}}(t)$  can be expanded as

$$|\Psi(t)\rangle = \sum_m c_m(t) |\psi_m\rangle \quad (\text{S24})$$

where  $|\psi_m\rangle$  ( $m = 0, 1, 2, \dots$ ) are the  $m$ th eigenstate of  $\hat{\mathcal{H}}$  with the eigenenergy  $\varepsilon_m$ . For simplicity, we assume that the ground state is not degenerate with  $\varepsilon_0 < \varepsilon_1 \leq \varepsilon_2 \leq \dots$ . By using the time-dependent perturbation theory, the coefficient  $c_m(t)$  is obtained as the sum over terms  $c_m^{(k)}(t)$  of the  $k$ th order expansion in terms of  $\hat{\mathcal{V}}(t)$ :

$$c_m(t) = \sum_{k=0}^{\infty} c_m^{(k)}(t). \quad (\text{S25})$$

Assuming that the initial state at time  $t_i = -\infty$  is the ground state  $|\psi_0\rangle$  of  $\hat{\mathcal{H}}$ ,  $c_m^{(k)}(t)$  is given as

$$c_m^{(k)}(t) = (-i)^k \int_{-\infty}^t dt_k \cdots \int_{-\infty}^{t_3} dt_2 \int_{-\infty}^{t_2} dt_1 \sum_{m_{k-1}} \cdots \sum_{m_2} \sum_{m_1} \langle \psi_m | \hat{\mathcal{V}}_I(t_k) | \psi_{m_{k-1}} \rangle \cdots \langle \psi_{m_2} | \hat{\mathcal{V}}_I(t_2) | \psi_{m_1} \rangle \langle \psi_{m_1} | \hat{\mathcal{V}}_I(t_1) | \psi_0 \rangle, \quad (\text{S26})$$

where  $\hat{\mathcal{V}}_I(t) = e^{i\hat{\mathcal{H}}t} \hat{\mathcal{V}}(t) e^{-i\hat{\mathcal{H}}t}$  [S9]. Because of Eq. (S20),

$$\langle \psi_m | \hat{\mathcal{V}}_I(t) | \psi_{m'} \rangle = \sum_{\mu} e^{i(\varepsilon_m - \varepsilon_{m'} - \mu\omega_p)t} \mathcal{V}_{mm'}^{(\mu)} \quad (\text{S27})$$

with

$$\mathcal{V}_{mm'}^{(\mu)} = \langle \psi_m | \hat{\mathcal{V}}^{(\mu)} | \psi_{m'} \rangle. \quad (\text{S28})$$

Therefore, we obtain for  $t \rightarrow \infty$  that

$$\begin{aligned} c_m^{(k)}(\infty) &= 2\pi i (-1)^k \sum_{\mu_k} \cdots \sum_{\mu_2} \sum_{\mu_1} \sum_{m_{k-1}} \cdots \sum_{m_2} \sum_{m_1} \mathcal{V}_{mm_{k-1}}^{(\mu_k)} \cdots \mathcal{V}_{m_2 m_1}^{(\mu_2)} \mathcal{V}_{m_1 0}^{(\mu_1)} \prod_{k'=1}^{k-1} \frac{1}{\varepsilon_{m_{k'}} - \varepsilon_0 - \left( \sum_{\ell=1}^{k'} \mu_{\ell} \right) \omega_p - i\gamma} \\ &\times \delta \left( \varepsilon_m - \varepsilon_0 - \left( \sum_{\ell=1}^k \mu_{\ell} \right) \omega_p \right), \end{aligned} \quad (\text{S29})$$

where  $\gamma \rightarrow 0^+$  is a convergence factor.

It is now obvious from the delta function in Eq. (S29)

that the coefficients  $c_m^{(k)}(t)$  for  $t \rightarrow \infty$  can be nonzero only if  $\varepsilon_m - \varepsilon_0 = (\sum_{\ell=1}^k \mu_\ell) \omega_p$ , suggesting that the excitations are allowed only to states with the excitation energy that is an integer multiple of  $\omega_p$ . This nicely explains the energy dependence found in Fig. 4(a) in the main text and Fig. S.3(a) for half-filling and also in Fig. S.5(a) away from half-filling. For example, if  $\sum_\ell \mu_\ell = 2\nu + 1$  ( $\nu$ : integer),  $\mathcal{V}_{mm_{k-1}}^{(\mu_k)} \cdots \mathcal{V}_{m_2 m_1}^{(\mu_2)} \mathcal{V}_{m_1 0}^{(\mu_1)}$  should involve the odd

number of excitations induced by the current operator  $\hat{J}$ . In the case of half-filling, combining this with the selection rule in Eq. (S17) yields that the  $\eta$  odd excitations are possible if and only if  $\varepsilon_m - \varepsilon_0 = (2\nu + 1)\omega_p$ . Similarly, the  $\eta$  even excitations are possible if and only if the  $\varepsilon_m - \varepsilon_0 = 2\nu\omega_p$  at half-filling. These are in accordance with the “tower of states” structure shown schematically in Fig. 4(c) in the main text.

---

[S1] T. J. Park and J. Light, *J. Chem. Phys.* **85**, 5870 (1986).  
 [S2] N. Mohankumar and S. M. Auerbach, *Comput. Phys. Commun.* **175**, 473 (2006).  
 [S3] H. Hashimoto and S. Ishihara, *Phys. Rev. B* **93**, 165133 (2016).  
 [S4] D. Pérez-García, F. Verstraete, M. M. Wolf, and J. I. Cirac, *Quantum Inf. Comput.* **7**, 401 (2007).  
 [S5] S. R. White, *Phys. Rev. Lett.* **69**, 2863 (1992).  
 [S6] U. Schollwöck, *Ann. of Phys.* **326**, 96 (2011).  
 [S7] M. P. Zaletel, R. S. K. Mong, C. Karrasch, J. E. Moore, and F. Pollmann, *Phys. Rev. B* **91**, 165112 (2015).  
 [S8] “<http://itensor.org/>”.  
 [S9] J. J. Sakurai, *Modern Quantum Mechanics* (Addison Wesley, 1993).  
 [S10] M. E. Rose, *Elementary Theory of Angular Momentum* (Wiley, New York, 1967).  
 [S11] S. Kitamura and H. Aoki, *Phys. Rev. B* **94**, 174503 (2016)